*Journal of Thermal Analysis, Vol. 44 (1995) 639-653*

# EFFECTS OF HYDROGEN AT HIGH TEMPERATURE ON $ZnAl_2O_4$ AND $Sn-ZnAl_2O_4$

*M. A. Valenzuela*[1,*], *P. Bosch*[2], *B. Zapata*[1], *G. Aguilar-Ríos*[1], *V. H. Lara*[2], *E. García-Figueroa*[2] *and I. Schifter*[1]

[1]Instituto Mexicano del Petróleo, A.P. 14805, 07730, México D. F., México
[2]Universidad Autónoma Metropolitana-I, A. P. 53534, 09340, México D. F., México

(Received January 7, 1994)

## Abstract

$ZnAl_2O_4$ and $Sn-ZnAl_2O_4$ were synthesized by coprecipitation, sol–gel and impregnation methods. These materials were calcined and treated in $H_2$ at 1073 K. Thermal analysis (DTA and TG), nitrogen physisorption (BET method), X-ray diffraction (XRD) and scanning electron microscopy (SEM) were used as characterization techniques.

$H_2$ treatment promoted $Al_xZn_y$ crystallization in the coprecipitated and impregnated samples. When tin was added to zinc aluminate, the tin acted as a protective shell against high-temperature reduction, independently of the preparation technique.

**Keywords:** high-temperature treatments, hydrogen effects, thermal analysis (DTA, TG), tin–zinc aluminate, zinc aluminate

## Introduction

Catalyst supports are generally metal oxides which must be stable in highly reducing environments [1, 2]. The reactivity of a metal oxide is often inhibited or, in some cases, promoted by the addition of transition metals. Reduction is accomplished either by removing lattice oxygen or by dissolving the reducing agent into the oxide lattice. Therefore, it depends on the presence of surface defects, bulk grain boundaries, the orientation of exposed surface planes, the presence of hydroxyl groups and, of course, the nature of the oxide [3].

Massoth and Scarpiello [4], reported the following sequence for the oxides, as concerns the ease of removal of oxygen at 200–600°C:

$$Fe_2O_3 > ZnFe_2O_4 > ZnCrFe_2O_4 = FeCrO_3 > ZnCr_2O_4 > ZnO > Cr_2O_3$$

---

[*] Presently at Instituto Politecnico Nacional-ESIQIE, Mexico

*0368–4466/95/ $ 4.00*

*John Wiley & Sons, Limited*
*Chichester*

The addition of zinc oxide to iron oxide causes a decrease in hydrogen consumption during the reduction process [5], and the reduction temperature shifts from 773 K to more than 973 K. However, in $ZnFe_2O_4$ treated at 813 K in a $H_2$ atmosphere, the iron is found to be reduced to the metal state and the ZnO, after reduction, is vaporized [4].

In ilmenite ($FeTiO_3$) treated with $H_2$ between 823 K and 1353 K, Briggs and Sacco [6] have demonstrated that iron forms a surface layer which inhibits hydrogen and water diffusion to the reaction front.

$ZnAl_2O_4$ has been shown to be a promising support for catalysts such as Pt and Pt–Sn because it stabilizes metal particles. If $ZnAl_2O_4$ is studied, no reduction is observed between 298 K and 973 K in a $H_2$ atmosphere [7]. However, a careful study of its thermal behaviour under reaction conditions has not yet been presented. Furthermore, the preparation technique may furnish solids with variable properties (surface area, for instance), which can be expected to behave differently.

In the present work, $ZnAl_2O_4$ and Sn–$ZnAl_2O_4$ prepared by coprecipitation and sol–gel methods were calcined at 1073 K and then treated in $H_2$ at 1073 K. The resulting reduced solids were compared with the calcined ones. For purposes of comparison, a sample obtained by the conventional impregnation of $ZnAl_2O_4$ with tin was also used.

## Experimental

### *Coprecipitated samples*

$ZnAl_2O_4$ samples were prepared by coprecipitation and sol–gel methods. In the first case, an aqueous solution of $Al^{3+}$ and $Zn^{2+}$ (atomic ratio Al:Zn = 2:1) was made from $Al(NO_3)_3{\cdot}9H_2O$ (Monterrey) and $Zn(NO_3)_2{\cdot}6H_2O$ (Baker). Precipitation was performed at variable *pH*, by adding a 50% vol. of aqueous $NH_4OH$ solution to the acidic mixed solution until *pH* 7.5 was attained. After washing and filtration, the obtained gel was aged for 24 h and dried in a vacuum oven at 383 K for 24 h. Calcination was carried out in a quartz tube in air flow. The heating rate was 10 $deg{\cdot}min^{-1}$, up to 1073 K; this temperature was maintained for 8 h.

Mixed oxides Sn–$ZnAl_2O_4$ were prepared by coprecipitation at variable *pH*. $SnCl_2{\cdot}2H_2O$ (Baker) was mixed with aqueous zinc and aluminum nitrate solutions, as in the preparation of $ZnAl_2O_4$. The Al:Zn atomic ratio was maintained at 2:1. The final tin content, measured by atomic absorption spectroscopy, was 1.6 wt%.

### *Sol–gel samples*

The $ZnAl_2O_4$ sol–gel sample was synthesized by dissolving aluminum tri-*sec*-butoxide (Aldrich) in isopropanol (the alcohol/alkoxide molar ratio was 60). The mixture was then added under continuous agitation to a vessel containing isopropanol at 343 K. The mixture was kept under reflux for 1 h. An aqueous solution of zinc nitrate with an aliquot of concentrated nitric acid was next added to the alcohol/alkoxide mixture. The water/alkoxide and acid/alkoxide molar ratios were 30 and 0.2, respectively. Refluxing was continued until

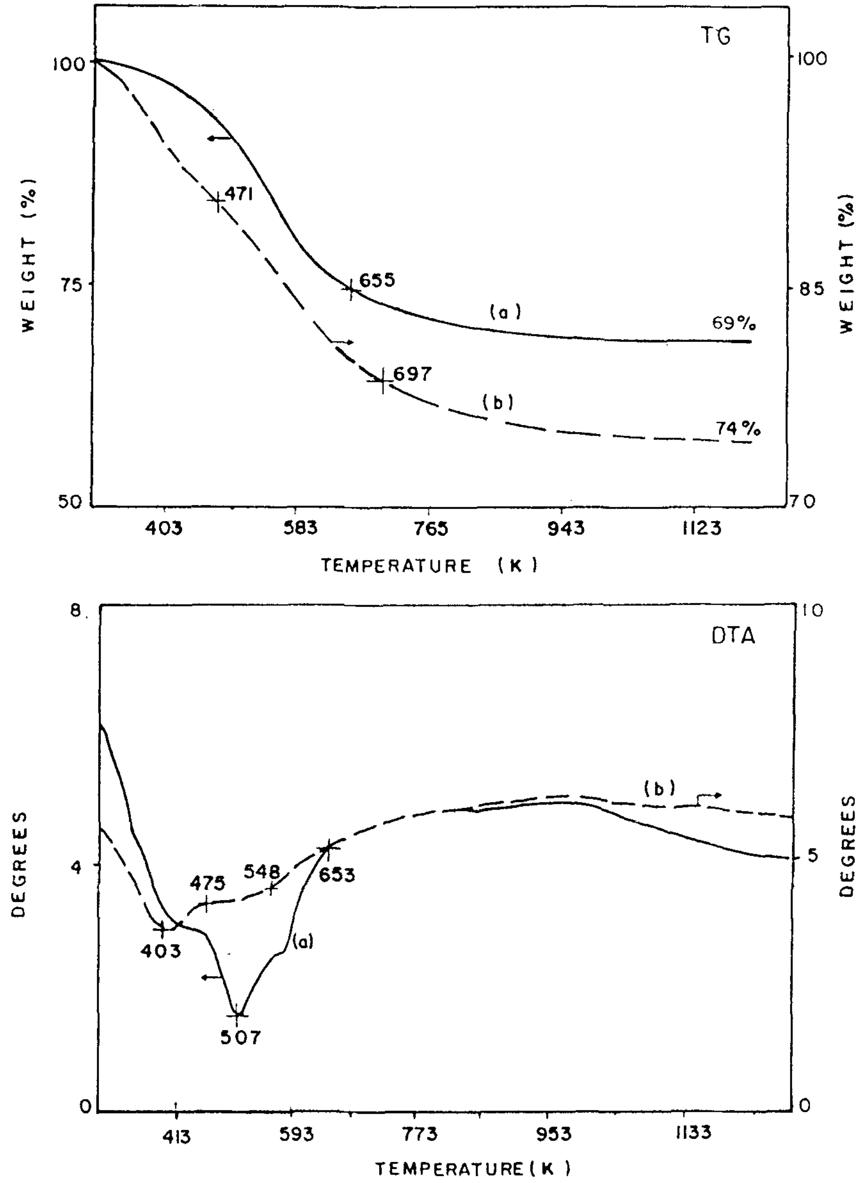

Fig. 1 TG and DTA curves of (a) $ZnAl_2O_4$ and (b) Sn–$ZnAl_2O_4$ coprecipitated dried gels

gelling occurred. The solvent excess was eliminated by distillation in vacuo. The obtained gel was aged for 24 h, and dried in a vacuum oven at 383 K for 8 h. Calcination was performed at 1073 K for 8 h.

The Sn–$ZnAl_2O_4$ sol–gel sample was synthesized as for $ZnAl_2O_4$ sol–gel sample. The gelling process was accomplished by addition of a mixture of tetrabutyltin (Aldrich), zinc nitrate, isopropanol, water and concentrated nitric acid to the alcohol/alkoxide mixture. The tin content, after calcining, was 1.8 wt.%.

### *Impregnated sample*

Coprecipitated $ZnAl_2O_4$ (calcined at 1073 K) was impregnated with an aqueous solution of tin chloride, and the water was eliminated in a rotary evaporator. The tin content was 1.5 wt.%. Calcined $ZnAl_2O_4$ and Sn–$ZnAl_2O_4$ samples were reduced in a $H_2$ flow for 4 h at 1073 K. The heating rate was 10 deg·min$^{-1}$ and cooling was performed without any program.

### *Characterization*

The crystallographic phases present in the samples were determined by X-ray diffraction with a Siemens D-500 diffractometer, using $CuK_{\bar{\alpha}}$ radiation and a diffracted beam monochromator. In some cases, the powders were mixed with an internal standard (α-alumina) and the corrected positions of the diffraction peaks were used to determine the cell parameters. Thermodiffractograms were obtained in situ with a temperature chamber operated at 5 deg·min$^{-1}$ in an air atmosphere from 298 K to 1073 K.

The BET surface area and pore volume were measured by isothermal desorption in adsorption/desorption measurements at 77 K, using nitrogen (Micromeritics ASAP-2000).

DTA and TG analyses were performed in DTA-1700 and TGS-2 Perkin Elmer instruments, respectively. The operation conditions were a heating rate of 10 deg·min$^{-1}$ and an air flow.

A Jeol scanning electron microscope (JSM-85 CF) equipped with Si–Li windows was used to obtain the micrographs of some selected samples.

## Results and discussion

### *Coprecipitated samples*

#### Treatment in air at 1073 K

TG curves of $ZnAl_2O_4$ and Sn–$ZnAl_2O_4$ are shown in Fig. 1a. There is no significant effect on the thermogravimetric behaviour when tin is added to

$ZnAl_2O_4$. The final loss for $ZnAl_2O_4$ was 31 wt.%, whereas for Sn–$ZnAl_2O_4$ it was 26 wt.% up to 1213 K. For both samples, a sharp decrease in mass is observed from room temperature up to around 673 K. This is attributed to the loss of water and residual nitrates. The loss in mass up to 673 K is attributed to the solid-state reaction yielding $ZnAl_2O_4$.

DTA curves of the samples are shown in Fig. 1b. For $ZnAl_2O_4$, a large endothermic peak is observed from room temperature up to 653 K. This behaviour confirms the TG results. For Sn–$ZnAl_2O_4$, the DTA curve exhibits one small endothermic peak in the same temperature range as for the $ZnAl_2O_4$ sample, with a minimum at 403 K. This reveals that Sn–$ZnAl_2O_4$ precursors retain some water, and therefore the water loss mechanism must be different.

In Table 1, the surface areas (*S.A.*), pore volumes (*P.V.*) and mean pore diameters (*M.P.D.*) of $ZnAl_2O_4$ and Sn–$ZnAl_2O_4$ are compared. It is found that addition of tin to $ZnAl_2O_4$ increases the surface area two-fold.

When $ZnAl_2O_4$ and Sn–$ZnAl_2O_4$ are calcined in an air flow (1073 K), the X-ray patterns correspond only to the $ZnAl_2O_4$ spinel structure. Figure 2 shows the $ZnAl_2O_4$ thermodiffractogram measured from room temperature up to 1073 K. The sharp and intense peaks at $2\theta=40.5°$, 47.1° and 68.9°, are due to the rhodium–platinum holder and may be used as a reference. Crystalline compounds are present from room temperature up to 373 K. The loss in mass at about 673 K can be interpreted due to the transformation of crystalline compounds to a $\gamma$-alumina-type structure. Dehydrated Zn compounds are then incorporated into the alumina, forming $ZnAl_2O_4$ [8]. This transition occurs at low temperature (873 K), but the well-crystallized spinel is obtained only at 1073 K. Low surface area and pore volume are observed. The Sn–$ZnAl_2O_4$ preparation displayed the same thermal behaviour as $ZnAl_2O_4$, but the precursors of Sn–$ZnAl_2O_4$ are not as well defined.

The solid-state reaction furnishing Sn–$ZnAl_2O_4$ begins at the same temperature (873 K) as in the sample without tin. Tin addition affects both the surface area and the pore volume, which are around double those reported for $ZnAl_2O_4$ (Table 1).

**Table 1** Results of the physisorption analysis of the coprecipitated $ZnAl_2O_4$ and Sn–$ZnAl_2O_4$ calcined samples

| Sample | *S.A.* / $m^2 \cdot g^{-1}$ | *P.V.* / $ml \cdot g^{-1}$ | *M.P.D.* / Å |
|---|---|---|---|
| $ZnAl_2O_4$ | 20 | 0.137 | 250 |
| Sn–$ZnAl_2O_4$ | 39 | 0.187 | 191 |

## Treatment in hydrogen at 1073 K

Figure 3 shows X-ray diffractograms of $ZnAl_2O_4$ and Sn–$ZnAl_2O_4$ treated in $H_2$ at 1073 K. Several differences may be observed for the $ZnAl_2O_4$ sample:

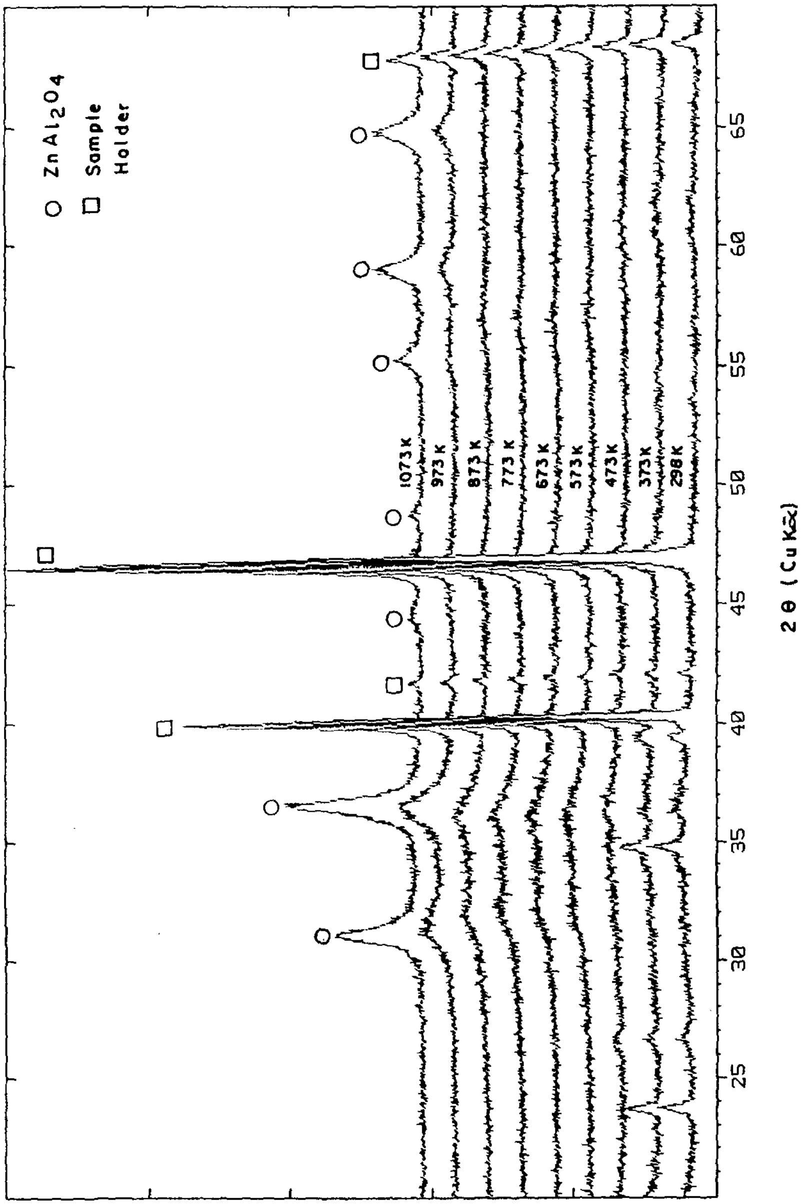

**Fig. 2** Thermodiffractograms of $ZnAl_2O_4$ coprecipitated dried gel

First, the (3 3 1) reflection with $d$=1.84 Å does not appear for the reduced material. Second, a small peak with $d$=2.28 Å is now observed, which can be attributed to $Al_{0.71}Zn_{0.29}$. Third, the cell parameter shifts to 7.95 Å, as compared with 8.08 Å for the calcined sample. In Sn–$ZnAl_2O_4$, the well-defined spinel structure is again present. After the reduction of this sample, a white-grey film was detected in the exit of the reactor. This section of the reactor was removed and analyzed by XRD, which revealed the presence of ZnO and $SnO_2$.

Figure 4 depicts the SEM image of the $ZnAl_2O_4$ coprecipitated sample reduced at 1073 K. Compressed and irregular 1 μ aggregates can be seen; the mean particle size is about 0.3 μ.

On $H_2$ treatment of $ZnAl_2O_4$, the (3 3 1) diffraction peak fades out, indicating that the sample may be preferentially oriented. Hence, the morphology of the crystals is altered by $H_2$ treatment. This conclusion is confirmed if the relative intensities of the diffraction peaks are considered: for instance, for calcined $ZnAl_2O_4$ (Fig. 3a) $I_{(220)}/I_{(331)}=0.71$, whereas for reduced $ZnAl_2O_4$ $I_{(220)}/I_{(331)}=0.48$. Therefore, the $H_2$ may follow the grain boundaries in selected crystallographic directions and it may react with $ZnAl_2O_4$ to produce $Al_{0.71}O_{0.29}$. In the case of Sn–$ZnAl_2O_4$, the spinel structure and the morphology are maintained, as $H_2$ reacts stoichiometrically with the spinel to form sublimed $SnO_2$ and ZnO. The resulting spinel must be zinc-deficient. Hence, tin addition stabilizes $ZnAl_2O_4$ and inhibits its reduction by $H_2$.

When $ZnAl_2O_4$ is treated in $H_2$, the $H_2$ apparently reacts with the large particles of $ZnAl_2O_4$ in a selective reduction of the particle size. Second, $H_2$ may modify the lattice composition, forming new compounds, such as $Al_{0.71}Zn_{0.29}$ (card ASTM 2–32). Third, $H_2$ removes lattice oxygen, selectively forming water. The particle morphology is also different, i.e. the $H_2$ reaction breaks down large particles. In the case of Sn–$ZnAl_2O_4$, the spinel structure is maintained. The $H_2$ reacts primarily with the $SnO_2$ surface particles and afterwards with the bulk, segregating ZnO.

### *$ZnAl_2O_4$ and Sn–$ZnAl_2O_4$ sol–gel samples*

#### Treatment in air at 1073 K

The TG and DTA curves of the $ZnAl_2O_4$ sol–gel sample are presented in Fig. 5. In the TG curve (Fig. 5a), there are three zones of mass loss: the first, from room temperature up to 483 K, corresponds to surface water removal; the second, in the range 483 K to 613 K, can be attributed to crystallization water loss; and the last, from 613 K to 1073 K, can be assigned to a dehydroxylation process to form $ZnAl_2O_4$. The total loss in mass (up to 1073 K) was 49.5%. Figure 5b shows the DTA curve of sol–gel $ZnAl_2O_4$. There are two well-defined endothermic peaks. The one at low temperature (330–473 K) is due to water re-

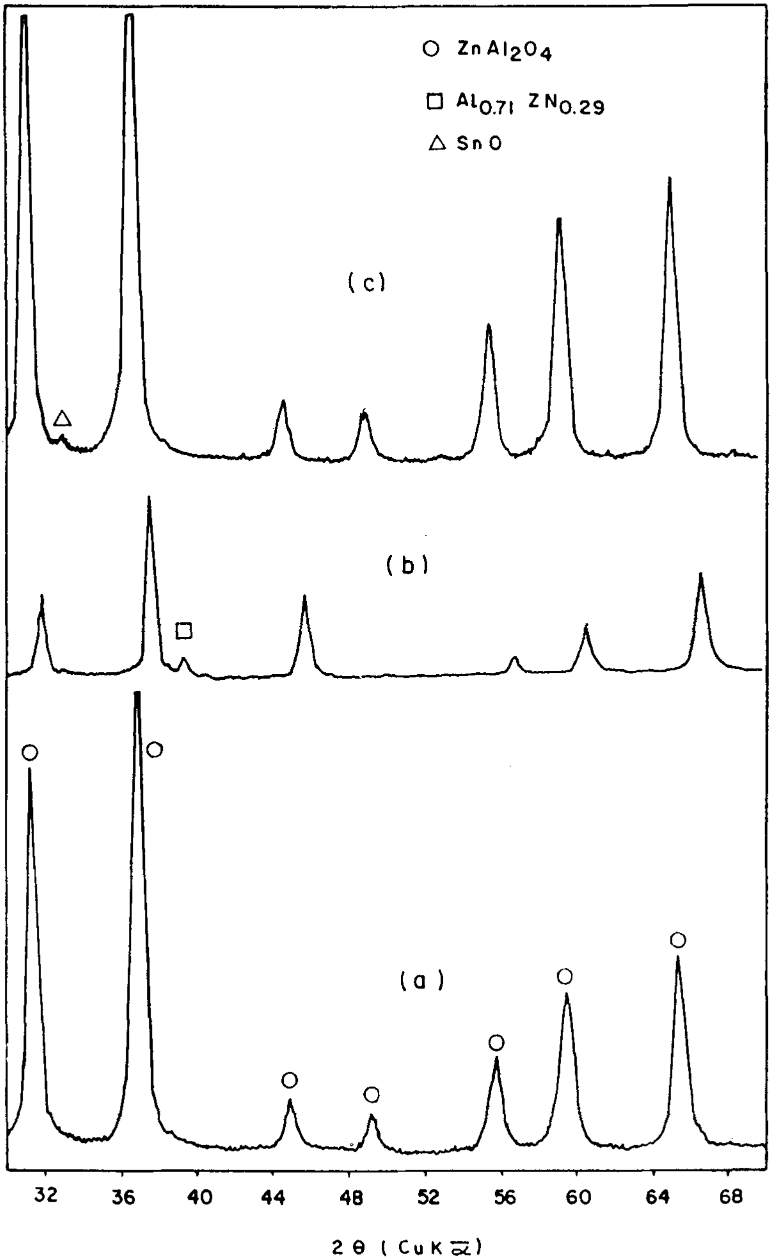

**Fig. 3** X-ray diffraction patterns of (a) $ZnAl_2O_4$ coprecipitated and calcined at 1073 K, (b) $ZnAl_2O_4$ coprecipitated, calcined at 1073 K and treated in $H_2$ at 1073 K, (c) Sn–$ZnAl_2O_4$ coprecipitated, calcined at 1073 K and treated in $H_2$ at 1073 K

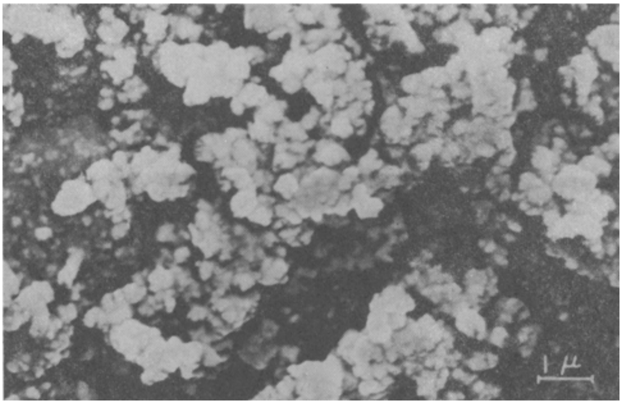

**Fig. 4** SEM image of $ZnAl_2O_4$ coprecipitated, calcined at 1073 K and treated in $H_2$ at 1073 K

moval. The broad endothermic peak in the range 483–613 K is due to the transformation of the initial crystalline compounds to γ-alumina [7].

Table 2 gives the $N_2$ physisorption results for $ZnAl_2O_4$ and Sn–$ZnAl_2O_4$. There are no significant differences between the two samples, but again the Sn–$ZnAl_2O_4$ sample has the higher surface area. If these results are compared with those for the coprecipitated samples (Table 1), it is clear that the sol–gel samples present different textural properties.

**Table 2** Results of physisorption analysis of the sol–gel $ZnAl_2O_4$ and Sn–$ZnAl_2O_4$ calcined samples

| Sample | *S.A.* / $m^2 \cdot g^{-1}$ | *P.V.* / $ml \cdot g^{-1}$ | *M.P.D.* / Å |
|---|---|---|---|
| $ZnAl_2O_4$ | 50 | 0.320 | 256 |
| Sn–$ZnAl_2O_4$ | 90 | 0.612 | 200 |

Figure 6 shows the thermodiffractogram of the sol–gel $ZnAl_2O_4$ from 298 K to 1073 K. If this is compared with Fig. 2, the crystallinity and the composition of the initial materials are seen to be different. As the temperature is increased, the compounds lose their order and become microcrystalline or amorphous, as in the case of coprecipitated $ZnAl_2O_4$. Further, the diffractograms at 773 K are similar for both preparations. The pattern may be attributed to γ-alumina.

However, at 973 K, the $ZnAl_2O_4$ in the coprecipitated sample is not fully crystallized; at the same temperature in the sol–gel preparation, $ZnAl_2O_4$ spinel has been synthesized, although the crystallite size must be small: the diffraction peaks are broad.

The cell parameter was determined for the sol–gel sample calcined at 1073 K ($a_o$=8.08 Å); no difference was found from the value obtained for the coprecipitated sample. It seems, therefore, that, independently of the initial reactants, an amorphous compound which crystallizes as a γ-alumina-like compound is needed. This γ-alumina-like structure, which is a spinel structure, crystallizes as $ZnAl_2O_4$ at high temperature.

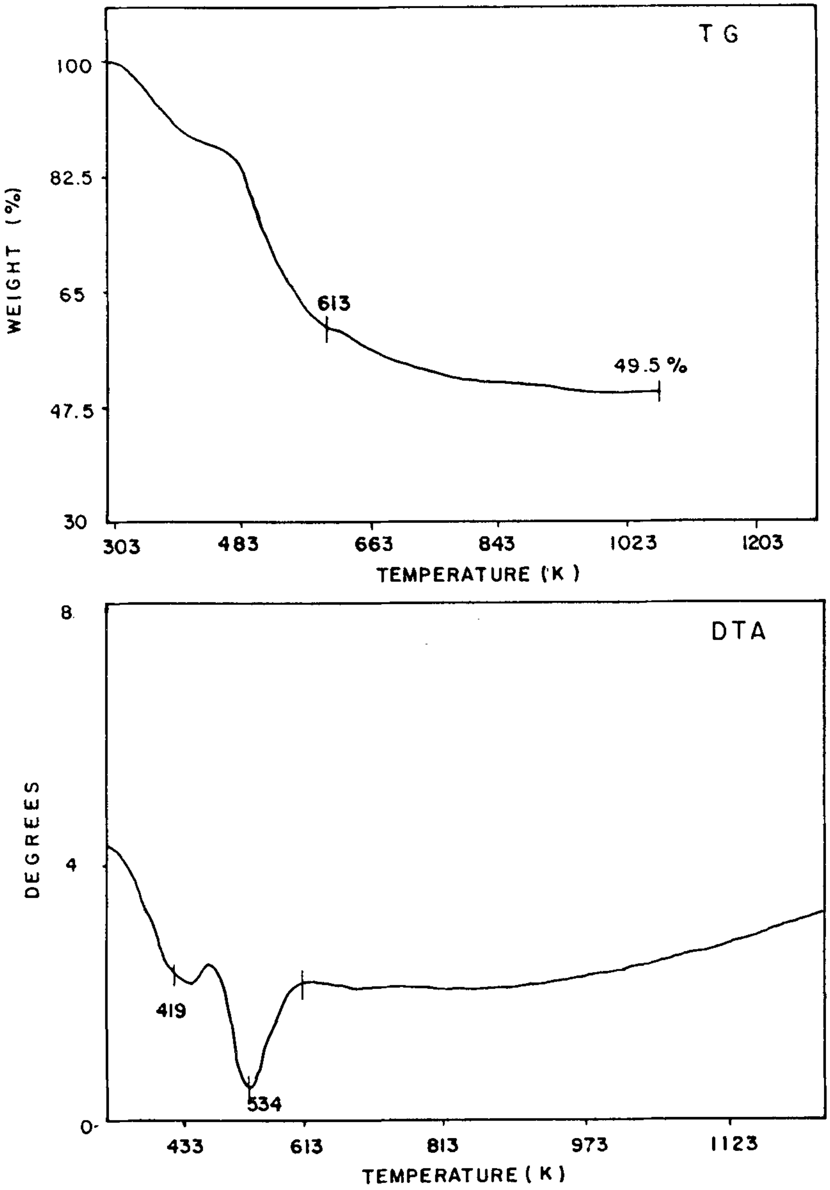

Fig. 5 TG and DTA curves of $ZnAl_2O_4$ sol–gel sample

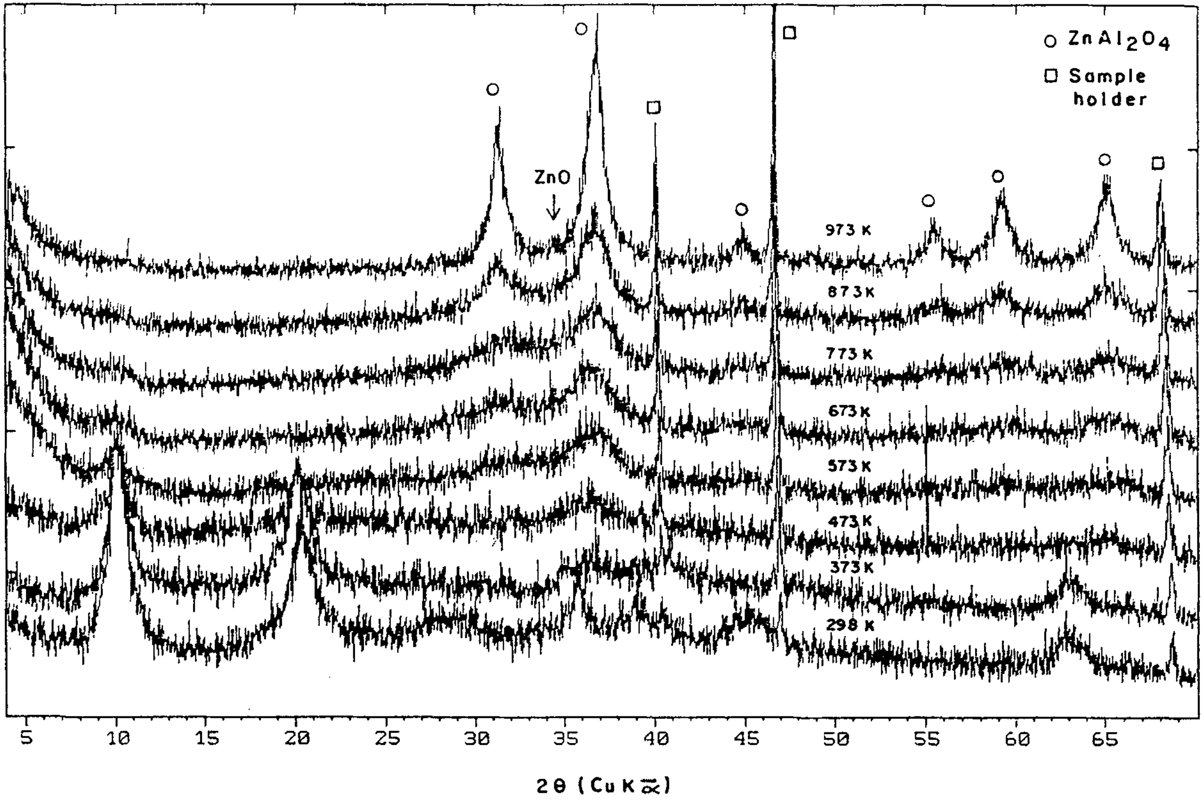

**Fig. 6** Thermodiffractograms of $ZnAl_2O_4$ sol–gel sample

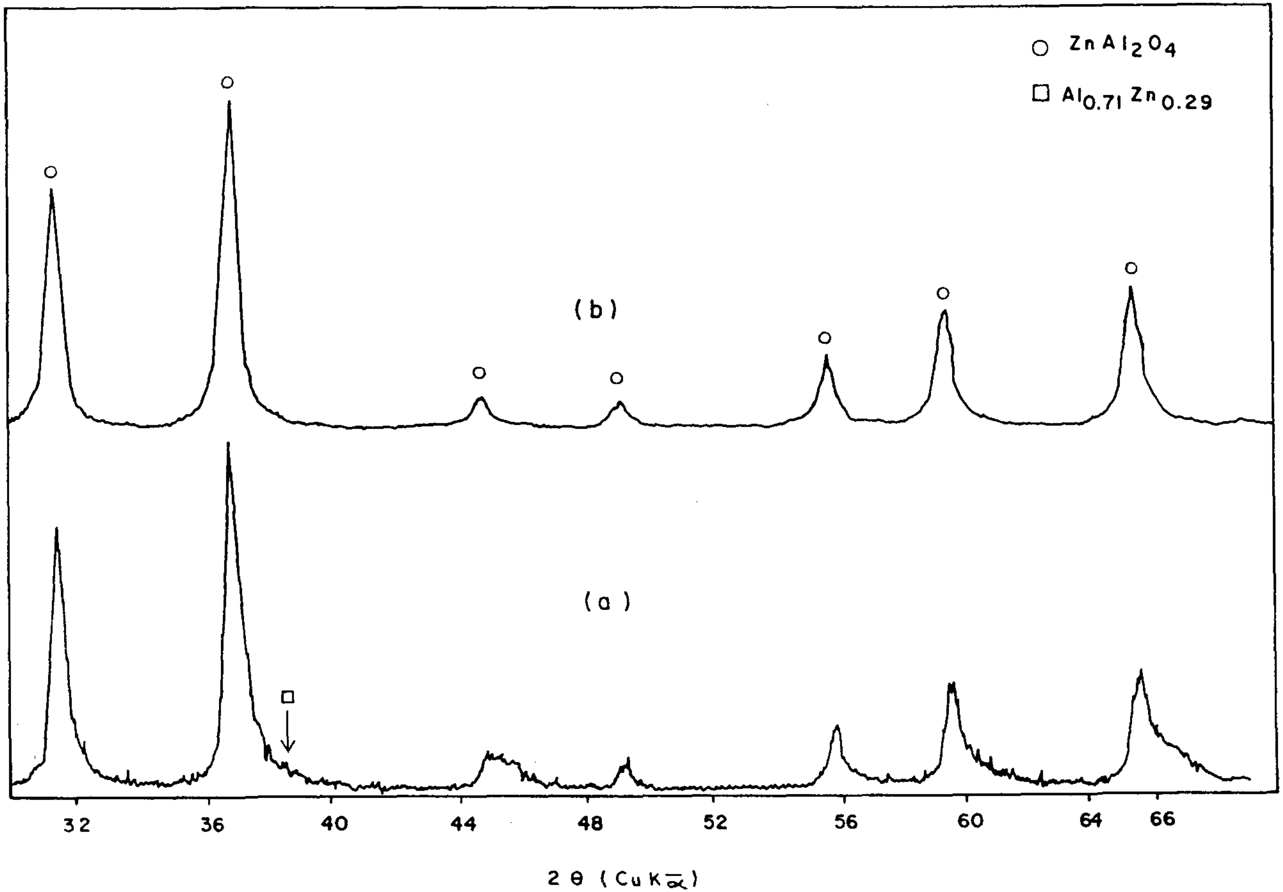

Fig. 7 X-ray diffraction patterns of (a) $ZnAl_2O_4$ and (b) Sn-$ZnAl_2O_4$. Sol-gel prepared samples, calcined at 1073 K and treated in $H_2$ at 1073 K

In the sol–gel preparation, nucleation centres are easily formed and hence the crystallite growth is homogeneous and rapid; this explains the lower crystallizing temperature. The crystal growth is probably also inhibited by the organic molecules present in the mixture. In the coprecipitated samples, the nucleation centres are fewer and they can grow by following the conventional mechanisms.

### Treatment in $H_2$ at 1073 K

Figure 7 shows diffractograms of the reduced $ZnAl_2O_4$ and Sn–$ZnAl_2O_4$ sol–gel samples. In the case of $ZnAl_2O_4$, the peaks are broad and double; this effect is clearly observed in the high angle peaks. A free ZnO phase is not present. A small peak is found at $d=2.32$ Å and can be attributed to $Al_{0.71}Zn_{0.29}$. In the Sn–$ZnAl_2O_4$ sample, the $ZnAl_2O_4$ spinel structure is maintained, and the amount of ZnO contained in the calcined sample has been reduced. Figure 8 depicts the SEM image of the sol–gel $ZnAl_2O_4$, calcined and reduced at 1073 K. If this image is compared with that of the coprecipitated sample (Fig. 4), several differences may be noted. First, the particle size is around 0.1 μ, and second, the particle aggregates are scarce.

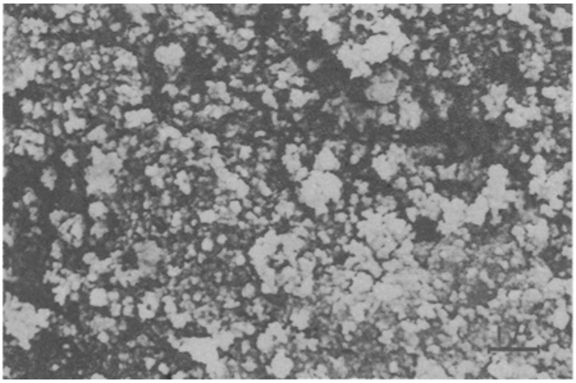

**Fig. 8** SEM image of $ZnAl_2O_4$ sol–gel prepared sample, calcined at 1073 K and treated in $H_2$ at 1073 K

## *Sn–$ZnAl_2O_4$ impregnated sample*

### Treatment in $H_2$ at 1073 K

Figure 9 shows the X-ray pattern of $ZnAl_2O_4$ impregnated with 1.5 wt.% tin and calcined at 1073 K. The X-ray diffractogram of this compound also displays broad and double peaks. The spinel structure is well defined and no other compounds are present excepting $Al_{0.71}Zn_{0.29}$. After the reduction step, $SnO_2$ but not ZnO was detected in the reactor effluent. Impregnation with tin seems

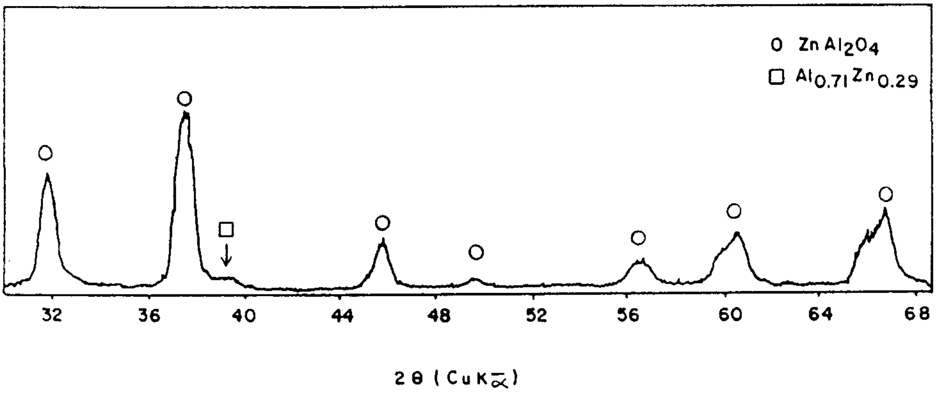

Fig. 9 X-ray diffraction pattern of Sn–$ZnAl_2O_4$ impregnated sample, calcined at 773 K and treated in $H_2$ at 1073 K

to provide a low tin interaction with the support. Tin is first reduced and then the support is attacked.

## Conclusions

In the present work, the following points emerge:

If tin is added to zinc aluminate, the tin acts as a protective shell against high-temperature reduction, independently of the preparation technique (excepting the impregnation method).

As far as the thermal behaviour is concerned, the coprecipitation and sol–gel preparations are equivalent.

$H_2$ treatment at 1073 K promotes $Al_xZn_y$ crystallization in coprecipitated and impregnated samples and ZnO in sol–gel samples. Sn compounds are reduced and swept out; they are condensed at the reactor exit. This shows that the amount of tin interacting with the support and acting as a protective shell is so low that it can be regarded as a surface dopant.

## References

1 A. B. Stiles, Symp. on Catalyst Supports, Am. Chem. Soc., N. York Meeting, August 25–30, 1991, p. 461.
2 L. J. Alvarez, J. F. Sanz, M. J. Capitán and J. A. Odriozola, Chem. Phys. Lett., 192 (1992) 463.
3 H. H. Kung, Transition Metal Oxides: Surface Chemistry and Catalysis, Elsevier Science Publishing Co., 1989, p. 91.
4 F. E. Massoth and D. A. Scarpiello, J. Catal., 21 (1971) 294.

5 H. Armendariz, G. Aguilar-Rios, P. Salas, M. A. Valenzuela and I. Schifter, Appl. Catal. A: General, 92 (1992) 29.
6 R. A. Briggs and A. Sacco, Jr., J. Mater. Res., 6 (1991) 574.
7 G. Aguilar-Rios, M. A. Valenzuela, H. Armendariz, P. Salas, J. M. Dominguez, D. R. Acosta and I. Schifter, Appl. Cat. A: General, 90 (1992) 25.
8 N. A. Pakhomov, O. P. Krivoruchko, L. M. Plyasova, S. V. Ketchik, R.A. Buyanov and G. R. Kotel'nikov, Kinet. i Katal., 25 (1984) 456.

**Zusammenfassung** — Mittels Kopräzipitation, Sol-Gel- und Imprägnierungsmethoden wurden $ZnAl_2O_4$ und $Sn-ZnAl_2O_4$ hergestellt. Diese Substanzen wurden kalziniert und in $H_2$ bei 1073 K behandelt. Zur Charakterisierung wurden Thermoanalyse (DTA und TG), Stickstoffphysisorption (BET Methode), Röntgendiffraktion und Scanning-Elektronenmikroskopie eingesetzt.
Die Wasserstoffbehandlung fördert die $Al_xZn_y$-Kristallisation in den kopräzipitierten und imprägnierten Proben. Wird dem Zinkaluminat Zinn zugesetzt, fungiert Zinn – unabhängig von der Herstellungsmethode – als Schutzschild gegen die Hochtemperaturreduktion.